RESEARCH ARTICLE Indian Journal of Animal Research, Volume 60 Issue 5: 807-815 (May 2026)

Screening of Intestinal Cytokines Differentially Expressed microRNAs in *Cryptosporidium parvum*-infected Mice

Liyun Chang[1,2#], Yanli Chen[3,4#], Qian Kang[2], Lixue Dong[4], Zhiyong Liu[4], Ying Li[4], Jianhua Qin[2]

10.18805/IJAR.BF-2009

ABSTRACT

Background: Cryptosporidium (*C. parvum*) is a kind of the intestinal tract that can cause diarrhea in humans and calves, however, the molecular mechanisms of host-parasite interactions are still poorly understood. Recently, non-coding microRNAs (miRNAs) have been identified as key regulators of host infection with parasites. This study aims to identify MicroRNAs molecules involved in *C. parvum* infection and immunity and to reveal their molecular mechanisms at the RNA level. This will provide a new idea for revealing the molecular mechanism of the relationship between trace small molecules and pathogenic infections.

Methods: It used bioinformatics analysis, qPCR and dual luciferase reporter test to investigate the miRNA expression profile of the posterior intestinal epithelium of Cryptosporidium-infected mice.

Result: The present study found that 204 microRNAs had differential expression in mice after infection with *C. parvum*, with 126 of them up-regulated and 78 of them down-regulated and quantitative real-time PCR validated partially differentially expressed microRNA (mmu-mi R-10, mmu-mi R-196, mmu-miR-27, mmu-miR-146, mmu-miR-145, mmu-mi R-21, let-7i and mmu-mi R-101), which consistented with high-throughput sequencing results. Different microRNAs were implicated in the pathways for Ras signaling, microbial infection, cancer, receptor interaction and the interaction of chemokine and cytokine receptors. By means of dual luciferase, TLR 11 was the target gene identified for miR-196, which indicated that MiR-196 may be involved in the host immune response to *C. parvum* through regulation of TLR-11. These results provide new insights into the regulatory mechanisms of host miRNAs during *C. parvum*, which may provide potential targets for future *C. parvum* control stmiceegies.

Key words: *C. parvum*, Differential expression, High-throughput sequencing, Luciferase report gene test, microRNA.

INTRODUCTION

C. parvum is a zoonotic parasite belonging to the phylum Apicomplexa. The parasite *C. parvum* has an genome, with eight chromosomes that range in size from 0.9 to 1.4 megabases (Rider *et al*., 2010). It can colonise gastroin-testinal epithelial cells and in calves it causes diarrhoea, dehydmiceion and emaciation which in severe cases can be fatal (Zolova *et al*., 2022). *C. parvum* is transmitted *via* the faecal-oral route. When *C. parvum* oocysts infect a person or animal, they release infectious sporozoites that attach to the intestinal epithelial cells and cause the development of parasitic vacuoles where *C. parvum* lives (Dixit *et al*., 2019; Li *et al*., 2021). Unlike other apicomplexan parasites, it is shielded from the unfavorable intestinal environment by utilizing parasitic vacuoles and provided with energy and nutrients by the host cell through a feeder organelle (Bouzid *et al*., 2014). In the digestive tract, new oocysts are produced through asexual or sexual reproduction and they are then expelled from the body to infect new hosts (Gallego *et al*., 2022). Pre-weaning calves are mainly infected with *C. parvum* (Shaw *et al*., 2021). However, the precise molecular pathogenic processes of *C. parvum* infection remain poorly known despite extensive research over the past years.

MicroRNAs (miRNAs) are highly conserved single-stranded non-coding RNAs of 21-23 nucleotides that play important gene regulatory roles in animals (Xie *et al*., 2021;

[1]Department of Life Science, Tangshan Normal University, Tangshan Key Laboratory of Animal Nutrition and Feed Engineering, Tangshan 063000, Hebei, China.
[2]College of Veterinary Medicine, Agricultural University of Hebei, Baoding 071000, Hebei, China.
[3]Tangshan Agricultural Science Research Institute, Thangshan 063001, Hebei, China.
[4]Tangshan Animal Disease Prevention and Control Center, Thangshan 063001, Hebei, China.
[#]These authors contributed equally to this work.

Corresponding Author: Ying Li, Jianhua Qin; Tangshan Animal Disease Prevention and Control Center, Thangshan 063001, Hebei, China; College of Veterinary Medicine, Agricultural University of Hebei, Baoding 071000, Hebei, China.
Email: 18232562315@163.com; qjhqqq@126.com
ORCIDs: https://orcid.org/0000-0001-9104-9464, https://orcid.org/0000-0001-7234-1304, https://orcid.org/0000-0002-8024-9871, https://orcid.org/0000-0002-4766-853x, https://orcid.org/0000-0002-7704-3610, https://orcid.org/0000-0003-3173-7091,https://orcid.org/0000-0001-8284-2110

How to cite this article: Chang, L., Chen, Y., Kang, Q., Dong, L., Liu, Z., Li, Y. and Qin, J. (2026). Screening of Intestinal Cytokines Differentially Expressed microRNAs in *Cryptosporidium parvum*-infected Mice. *Indian Journal of Animal Research*. **60(6):** 807-815. doi: 10.18805/IJAR.BF-2009.

Submitted: 14-04-2025 **Accepted:** 08-07-2025 **Online:** 19-07-2025

Khandelwal *et al*., 2024), including regulating immune cells, affecting the integrity of the intestinal epithelial barrier, participating in epithelial cell development and influencing the intestinal flor (Xiao *et al*., 2022). For example, Some microRNAs have been demonstmiceed to participate in *C. parvum* infection and to control the epithelial cells' immunological response to *C. parvum* in a particular way. Through the use of TLR2/TLR4/NF-B channels, *C.parvum* -infected organisms enhanced the expression of miR-942-5 p in HCT-8 cells (Xie *et al*., 2022); Let-7 can contribute to the epithelial cell defense mechanism brought on by *C. parvum* infection by triggering TLR4 signaling and increasing SNAP23 expression (Hu *et al*., 2013). Currently, although some studies have revealed changes in miRNA expression profiles after sporozoite infection of intestinal epithelial cells, there are no well-established reports on changes in microRNA expression profiles in in vivo models of *C. parvum* infection. Recently, to determine the interactions between microRNAs and their target genes, single or dual-luciferase reporter systems are frequently used (Deng *et al*., 2022). High-throughput sequencing methods and bioinformatics are also widely used for microRNA identification and differential expression analysis (Jeseninik *et al*., 2022).

MATERIALS AND METHODS

Parasites strain and test animals

The *C. parvum* oocysts were kept by the Labomiceory of Preventive Veterinary Parasitology, College of Animal Medicine, Hebei Agricultural University; 48 three-week-old SPF-grade female Balb/c mice were purchased from Vitalriver, Beijing, China.

Establishment of BALB/c mice model infected with *C. parvum*

The animal and environment were disinfected thoroughly before the experiment. The setting in which mice are housed is sterile and drinking water is sanitized by boiling. Forty-eight female BALB/c mice (weigh: 11 g-14 g) aged 3 weeks, after 3 days of feeding adaptation, microscopic examination of mice feces confirmed no parasitic infection were randomly divided into four groups, namely two infection groups with 12 mice in each group, two control groups with 12 mice in each group, One of the groups for intestinal tissue extraction and another group for collection of mice feces, weighing and dissection.

Oral drinking water with the 15 mg/mL of dexamethasone acetate and 40 mg/L of gentamicin were used for immunosuppression for 7d. We use gastric lavage needles to administer orally. Artificial gavage of *C. parvum* 1.0×10^5/mL oocyst suspension was administered twice at 500 µL each on an empty stomach. Mice feces were collected daily after infection, starting on the first day and were detected under a microscope and with acid-fast staining.

The present study was researched in agreement with the institutional and national guidelines and was supported by the Animal Use and Ethics Committee of the Agricultural University of Hebei (University Identification Number: HB/2023/03).

MicroRNA sequencing and differential expression analysis

Small intestine tissue was taken from mice infected with *C. parvum* one week after infection and total RNA was extracted. The purity of RNA was detected by formaldehyde denatured agarose gel and Nanodrop. Then, Qubit and Agilent 2100 were used to detect the concentration and integrity of RNA. After pooling the different libraries according to the effective concentration and the amount of target offline data, they were sent to Beijing Nuohe Source Sequencing Company for HiSeq sequencing and analysis. concentration.

Differential microRNA target gene enrichment analysis

Prediction of microRNA target genes by intersection of miRanda, PITA and RNAhybrid, Gene Ontology and KEGG enrichment analysis were performed on the set of different microRNA-expressing target genes according to the correspondence between microRNA and its target genes. The most important biochemical metabolic pathway and signal transduction pathway in which the candidate gene is involved can be determined by significant enrichment analysis.

Validation of differentially expressed microRNAs

MicroRNAs that were differentially expressed were confirmed using real-time quantitative PCR. The volume of reaction mixtures was 20 µL, containing 2 µL cDNA, 10 µL trans start tip green qPCR super mix (Trans gen biotech, China), 0.4 µL forward primer (0.2 µM), 0.4 µL reverse primer (0.2 µM) and 7.2 µL dd H_2O. MicroRNA primers are shown in Table 1. The following amplification program was used: pre-denatumiceion at 95°C for 10 min, followed by a total of 45 cycles, consisting of denatumiceion at 95°C for 30 s, annealing at 60°C for 20 s and extension at 72°C for 20 s. The expression level was calculated using $2^{-\Delta\Delta Ct}$ method and normalized by the reference gene.

Table 1: Design and synthesis of primers for microRNAs.

Primer	Primer sequence
mmu-miR-21a-5p F	GCGTAGCTTATCAGACTGATGTTGA
mmu-miR-196-5p F	CGTAGGTAGTTTCATGTTGTTGGG
mmu-miR-101a-3p F	CGCGTACAGTACTGTGATAACTGAA
mmu-miR-27a-3p F	AGTTCACAGTGGCTAAGTTCCGC
mmu-miR-146a-3p F	CGCTGAGAACTGAATTCCATGGGTT
mmu-miR-145a-5p F	GTCCAGTTTTCCCAGGAATCCCT
mmu-miR-16-5p F	CCGTAGCAGCACGTAAATATTGGCG
mmu-miR-10-5p F	CGTACCCTGTAGATCCGAATTTGTG
mmu-let-7a-5p F	GCGTGAGGTAGTAGGTTGTATAGTT

Verification of miR-196 regulating TLR-11 gene

Prediction of microRNA target genes

By combining the functions of the programs microRNAmi Randa, PITA and RNAhybrid, the microRNA target genes were predicted. The primary biochemical metabolic pathways and signal transduction pathways involved in potential target genes were identified using Gene Ontology and KEGG enrichment analysis in conjunction with the correlation between microRNA and its target genes.

Construction of TLR-11 3′ -UTR target gene vector

According to microRNA target gene prediction results, the correspondence between microRNA and target gene was analyzed.

miR-196 was increased by 135.85 times and it was related to the toll-like receptor signaling pathway by simultaneous association analysis. Bioinformatics analysis predicts that there may be a site that is not completely complementary to miR-196 at the 2932-2954 base position of the 3′-UTR of TLR-11 mRNA gene, as shown in Fig 1. According to the prediction results, a 162-base sequence that may contain a complementary binding site with miR-196 was designed and synthesized. At the same time, a 3′ -UTR base mutation chain gene sequence of the TLR-11 mRNA gene that may contain a complementary binding site with miR-196 was designed and synthesized. The Xho I restriction endonuclease site was added to the 5′ end and 3′ end of the target fragment. The designed and synthesized gene sequence is as follows.

TLR-11 3′-UTR base normal strand (176 bp)

5′**CCTCGAG**AGCTGGACAAGAAAGAGATTAAG GACTGCAGGAATGCTGTTGTGCAGAAGATCCTTTCAG CAGCAGAGGGAATGTGCTCTCATCACTAAAGCATGG GCTCACCAAGGGGGCAAAATGATATATTAAATTCC ACTGGGAGAGAAGTCTTTTAAAACACTGAAA**CTCGAGT**3′

TLR-11 3′-UTR base mutation strand (176 bp)

5′**CCTCGAG**AGCTGGACAAGAAAGAGATTAA GGACTGCAGGAATGCTGTTGTGCAGAAGATCCTTAG TCGTCGTGAGGGAATGTGCTCTCATCACTAAAGCA TGGGCTCACCAAGGGGG CAAAATGATAT ATTAAATTCCAC TGGGAGAGAAGTCTTTT AAAACACTGAAA**CTCGAGT**3′

The 3′-UTR sequence of the target gene TLR-11 of miR-196 was inserted into the MCS downstream of the firefly luciferase reporter vector gene and part of the 3′ non-coding region of TLR-11 was ligated to the pmir-GLO vector. Renilla luciferase gene was used as internal reference gene.

Identification of target gene vector by enzyme digestion

The pmir-GLO vector was transferred into the receptor cell Mch1T1 strain and incubated at 37°C for 12-15 h. After incubation on medium containing AMP, monoclonal colonies were picked and incubated for 12 h-15 h. The plasmids were extracted using the Plasmid Extraction Kit. The successful ligation was verified with Xho I restriction endonuclease and operate according to the Thermo Fisher (USA) enzyme digestion kit instructions. The reaction solution after enzyme digestion was examined by agarose gel electrophoresis.

Culture and transfection of 293T cells

The experiments were divided into 4 groups: TLR-11 3′-UTR+miR-196mimic group; TLR-11 3′-UTR+miR-196 NC group, TLR-11 mut-3′-UTR+miR-196mimic group, TLR-11 mut-3′-UTR+miR-196 NC group. The assay was conducted in a 24 well plate. Firstly, 293T cells were cultured in 37°C, 5% carbon dioxide and satumiceed humidity and the culture medium was removed when they grew to 80%. Then 500 μL of Opti-MEM reduced serum medium was added to each well and incubate for 2 h. The TLR-11 3′-UTR+miR-196mimic group was loaded with 0.25 ug miR-196mimic and TLR-11 3′-UTR, TLR-11 3′-UTR+miR-196 NC group was loaded with 0.25 ug miR-196 NC and TLR-11 3′-UTR, the TLR-11 mut-3′-UTR+miR-196mimic group was loaded with 0.25 ug TLR-11 mut-3′-UTR and miR-196mimic, TLR-11 mut-3′-UTR+miR-196NC group was loaded with 0.25 ug TLR-11 mut-3′-UTR and miR-196NC and each well was added 1.5 μL liposome 2000, 548.5 uL Opti-MEM reduced

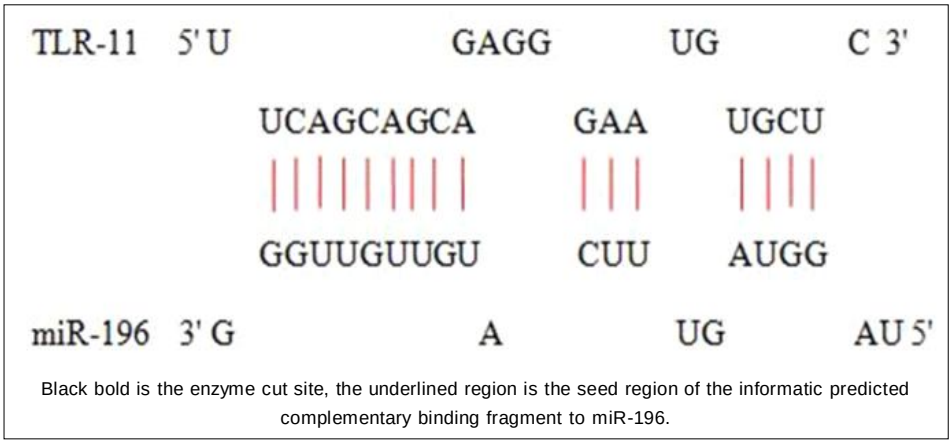

Black bold is the enzyme cut site, the underlined region is the seed region of the informatic predicted complementary binding fragment to miR-196.

Fig 1: Binding site of miR-196 and TLR-11 mRNA gene.

serum medium, Mix up all components. The cells were inspected under a microscope after incubated for 24 and 48 h.

BiLuciferase reports experimental validation of target gene activity

The sea kidney fluorescence luminescence value and the firefly fluorescence luminescence value were detected by a multifunctional microplate reader in accordance with the dual luciferase reporter gene detection system kit's instructions. The following formula was used to compute the relative fluorescence activity:

$$\text{Relative fluorescence activity} = \frac{\dfrac{\text{Firefly fluorescence activity}}{\text{Sea kidney fluorescence activity (test group)}}}{\dfrac{\text{Firefly fluorescence activity}}{\text{Sea kidney fluorescence activity (treatment group)}}}$$

Institutional review board statement

All the experiments were approved by the appropriate ethics committees of Hebei Agricultural University.

RESULTS AND DISCUSSION

Observation results of BALB/c Mice After Infection with *C. parvum*

Poor mental functioning, lack of appetite, decreased activity, piloerection and decreased skin elasticity were all observed in the mice. As shown in Fig 2, The mice in the experimental group gained weight more slowly than these in the control group. Four mice perished two weeks after infection. All of the dead mice experienced dyspnea, generalized shaking, dehydmiceion and body emaciation prior to passing away. The small intestine's intestinal chyme was yellow and fluid, the stomach was swollen and the intestinal wall was thin and inflated, according to the autopsy. As shown in Fig 3, red arrows in the figures point to *C. parvum* after acid fast staining under a microscope and without acid fast staining.

After intragastric administration of *C.parvum* oocysts, fresh mouse feces were collected every day. Fecal samples were filtered and centrifuged and the oocyst output was observed by Maxwell's counting method. The overall change was in a wave shape as shown in Fig 4. On 1st day, oocysts were detected from feces and the output of oocysts was

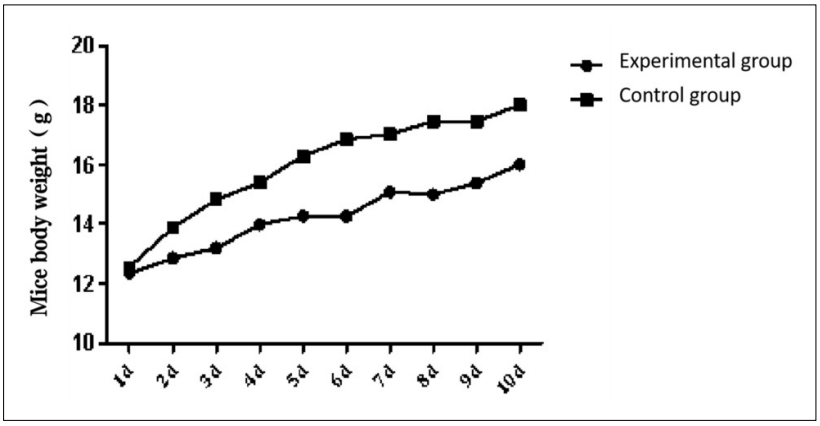

Fig 2: Mouse body weight changes.

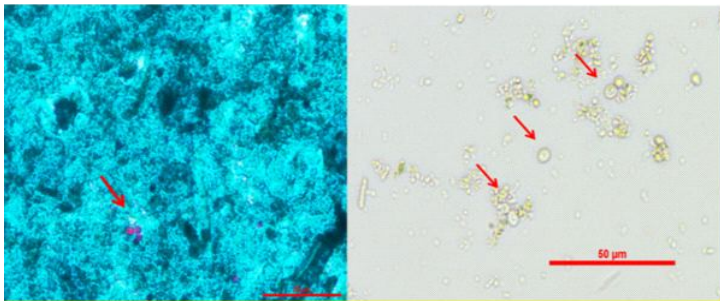

The right image displays the microscopic examination of *C. parvum* at the unstained stage under 400 times magnification. The left image shows the microscopic examination of *C. parvum* after acid-fast staining.

Fig 3: The images were obtained microscopically for *C. parvum.*

relatively large, due to part of the oocysts being excreted with feces after gavage infection; the number of oocysts increased significantly on the 3rd day. The peak of output was 7-11 dpi and reached the top on the 9th day. After that, oocysts were continuously discharged until the 14th day.

HiSeq sequencing and analysis results

MicroRNA sequencing results

A total of 656 microRNA precursors and 812 microRNA matures were found and 15 new matures and 15 new precursors were predicted. And the details are shown in Table 2. What's more, the results showed that there were 204 differentially expressed microRNAs, of which 126 were up-regulated and 78 were down-regulated (Table 3).

Results of microRNA differential expression analysis

The results of microRNA differential expression analysis based on sequencing and analysis are shown in Table 4. The expression of microRNA of let-7 family, mmu-miR-10, mmu-miR-196, mmu-miR-146 and mmu-miR-145 in the experimental group were significantly higher than those in the control group. When compared to the control group, the expression was significantly lower in mmu-miR-21, mmu-miR-27and mmu-miR-101. The results indicated that the expression of microRNA changed after *C. parvum* infection.

Screening of differential microRNAs

According to the microRNA difference fold and q.value in the sequencing results, the evaluation was performed. The overall distribution of small differential RNAs is shown in Fig 5. The horizontal and vertical axes indicate the expression and statistical significance of microRNAs in different experimental groups, respectively. The microRNAs with no significant difference were expressed in blue and the differentially up-regulated microRNAs were expressed in red, with 126; down-regulated significantly differential microRNAs were expressed in green, with 78.

Differential microRNA target gene enrichment analysis

The results of Geneontology (GO) enrichment analysis and KEGG Pathways enrichment analysis of differential microRNA target genes are shown in Fig 6, According to the enrichment analysis of microRNA target genes, indicating that differential microRNAs are involved in Ras signaling pathway, microbial infection, cancer pathway, receptor interaction pathway and chemokine and cytokine receptor interaction.

Verification of differentially expressed microRNAs

Using miR-16 as the internal parameter, real-time fluorescence quantitative RT-qPCR detection was performed and the differential expression microRNA (mmu-miR-10, mmu-miR-196, mmu-miR-27, mmu-miR-146, mmu-miR-145, mmu-miR-21, let-7i and mmu-miR-101) in sequencing results were randomly selected for verification. These results were consistent with the results of high-throughput sequencing, as shown in Fig 7. Let-7i can regulate NF-κB activation by modifying SIRT1 protein expression and participate in NF-κB-mediated epithelial innate immunity (Xie *et al.*, 2014; Yin *et al.*, 2021). Furthermore, the production of TLR4 in bile duct cells, which let-7i can control, can help the epithelial immune system respond to the *C. parvum*

Table 2: The number of microRNA mature bodies and precursors.

Types	Total	Control group	Experimental group
Known mapped mature	812	697	690
Known mapped hairpin	656	564	580
New mapped mature	15	11	12
New mapped hairpin	15	11	13

Table 3: Number of differential microRNAs.

Group	DIFF	UP	Down
Eg1vsCg2	204	126	78

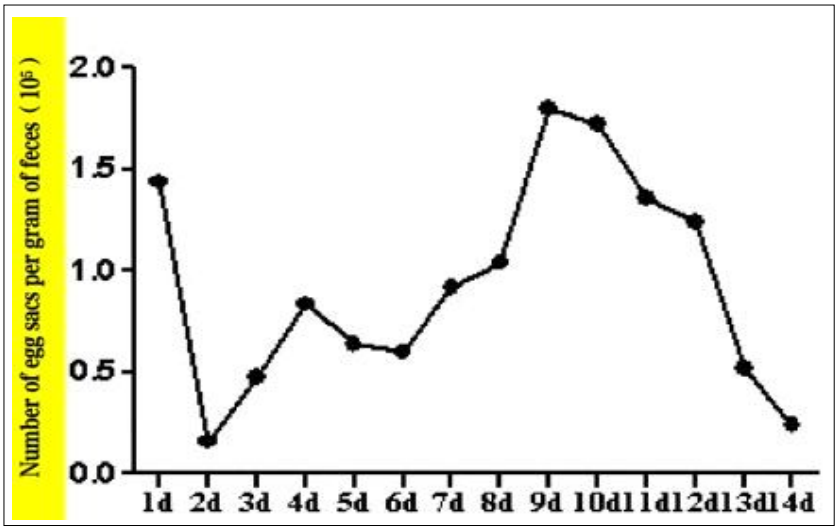

Fig 4: Changes in the discharge of oocysts.

infection. Therefore, let-7i may be associated with antigen presentation and T cell activation. The expression of let-7 family was significantly higher in the test group compared to the control group in this experiment ($P<0.01$) and it is speculated that let-7 may be involved in the innate and cellular immune responses of *C. parvum*.

The expression of miR-146 was significantly decreased in this experiment, which may further cause the positive regulation of toll-like receptors, while TLR2 and TLR4 are involved in the recognition of microscopic *C. parvum* by the intestinal mucosa, which may be one of the mechanisms of host resistance to *C. parvum* infection. Recently, a study found that Knockdown of miR-21 inhibits NLRP3 inflammasome-mediated caspase-1 activation and IL-1β secretion in macrophages (Nahand *et al*., 2021). *C. parvum* can evade clearance by the host immune system by inhibiting host cell apoptosis (Crawford *et al*., 2021). In this study, the expression of miR-21 was reduced. The occurrence of this change may be due to the fact that after host infection with *C. parvum*, the organism regulates the low expression of miR-21 to promote apoptosis, attenuate the oxidative stress caused by NLRP3, alle*vi*ate tissue damage and further promote the parasite clearance effect. This may be one of the mechanisms of action for host clearance of immune parasite infections.

Verification results of miR-196 on TLR-11 gene regulation

Target gene prediction results

The correspondence of known microRNA target gene was obtained by miRanda, PITA and RNAhybrid analysis and bioinformatics analysis predicted. In the 2932-2954 base position of TLR-11 mRNA gene 3′-UTR, there may be a site that is not completely complementary to miR-196. The known microRNA target gene prediction results show that the target gene of miR-196 may be TLR-11 and the up-regulation of miR-196 may affect TLR-11 expression.

Table 4: Partial results of microRNA differential expression analysis.

microRNA	Eg1	Cg2	log2.Fold_change	p.value	q.value
mmu-let-7a-5p	10320.32259	2942.157258	1.8105	0	0
mmu-let-7b-5p	17254.02415	3081.359557	2.4853	0	0
mmu-let-7c-5p	26953.59479	9378.453144	1.5231	0	0
mmu-let-7d-5p	3126.388649	982.4624674	1.67	0	0
mmu-let-7e-5p	1886.941924	284.4393794	2.7299	0	0
mmu-miR-100-5p	2009.85801	838.0300244	1.262	0	0
mmu-miR-101a-3p	160.4594931	3141.305056	-4.2911	0	0
mmu-miR-10a-5p	40534.02227	12417.56923	1.7068	0	0
mmu-miR-10b-5p	11188.44959	3136.074911	1.835	0	0
mmu-miR-27-3p	4904.814698	1140.976068	2.1039	0	0
mmu-miR-142a-5p	18.00026365	2065.102312	-6.8421	0	0
mmu-miR-143-3p	55066.40655	149562.8121	-1.4415	0	0
mmu-miR-145a-5p	15583.08539	6617.339338	1.2357	0	0
mmu-miR-146a-3p	45607.52515	128571.8296	-1.4952	0	0
mmu-miR-151-3p	5244.762534	836.4207493	2.6486	0	0
mmu-miR-181a-5p	4386.921398	1751.293661	1.3248	0	0
mmu-miR-192-5p	27155.71203	119988.3584	-2.1436	0	0
mmu-miR-194-5p	61705.41808	187177.2044	-1.6009	0	0
mmu-miR-1981-5p	1913.170879	232.5402564	3.0404	0	0
mmu-miR-200a-3p	5484.93748	18072.96436	-1.7203	0	0
mmu-miR-200b-3p	30084.61208	14615.03442	1.0416	0	0
mmu-miR-200c-3p	12922.64642	4982.718124	1.3749	0	0
mmu-miR-203-3p	847.5552712	7507.670804	-3.147	0	0
mmu-miR-215-5p	38723.71004	289286.1138	-2.9012	0	0
mmu-miR-21a-5p	21023.79365	125959.5738	-2.5829	0	0
mmu-miR-30e-5p	589.8943544	6010.642614	-3.349	0	0
mmu-miR-375-3p	8029.660467	3719.034827	1.1104	0	0
mmu-miR-378a-3p	52307.73758	23493.80764	1.1547	0	0
mmu-miR-423-3p	1833.969719	513.3587668	1.8369	0	0
mmu-miR-99a-5p	2701.582427	920.1030561	1.5539	0	0
mmu-miR-99b-5p	2080.830478	999.3598563	1.0581	0	0

*Note: [a]microRNA: MicroRNA maturing. [b]Eg1: Test group. [c]Cg2: Control group. [d]log2. Fold_change: Fold difference in expression between samples (Sample1/Sample2). [ef] q.value: The smaller the corrected p.value and q.value, the more significant the difference in microRNA expression.

Results of enzyme digestion identification of target gene vector

The plasmid digested by Xho I restriction endonuclease was detected by 1.5% agarose gel electrophoresis and the strips of 7350 bp and 176 bp sizes can be seen as shown in Fig 8. This proves that the pmir-GLO vector has been joined to both the normal TLR-11 mRNA gene 3′-UTR chain and the TLR-11 mRNA gene 3′-UTR mutant chain.

Dual luciferase reporter assay verified the prediction results of miR-196 target genes

Statistical analysis was conducted on all data using SPSS 22.0 software and t-test analysis was used to analyze the data. P≤0.05 was considered significant.The target gene of miR-196 was predicted by RNAhybrid and Targetscan and it was found that the target gene was TLR-11. In the comparison test of transfection of recombinant plasmid

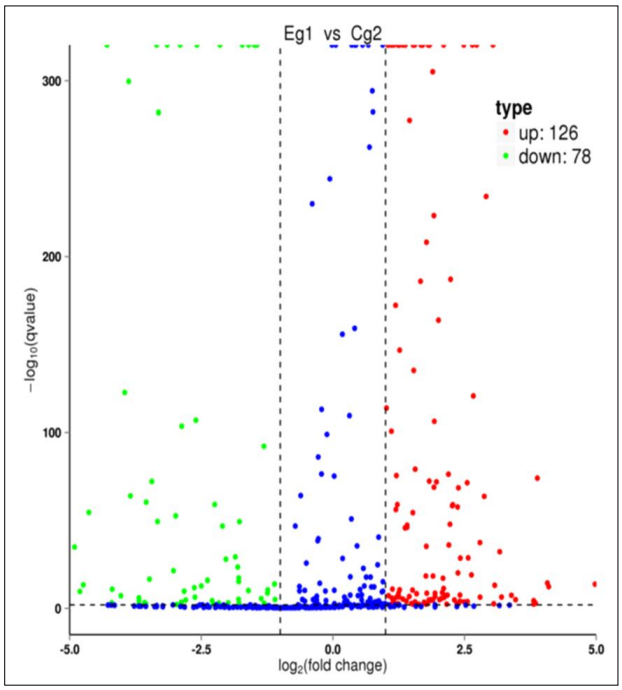

Fig 5: Overall distribution of differential microRNAs.

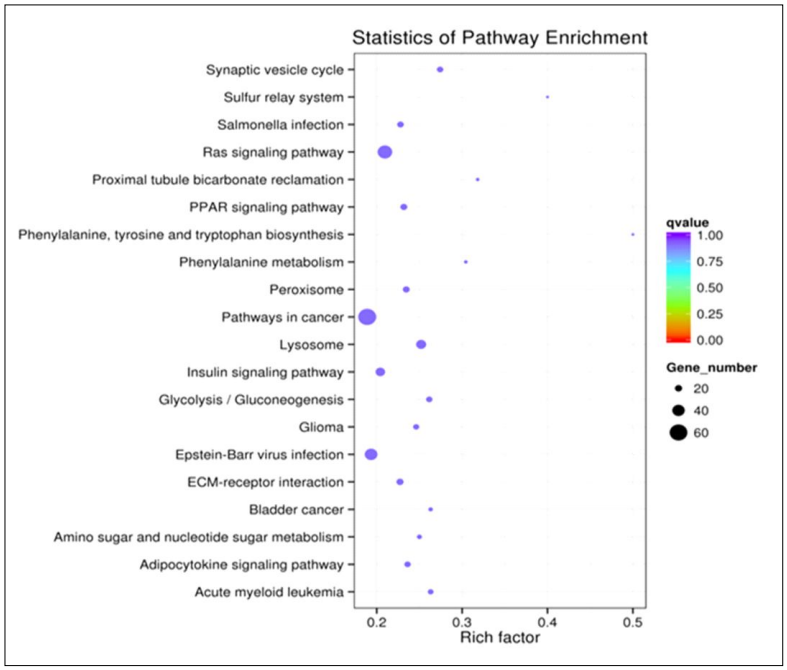

Fig 6: Differential microRNA target gene enrichment analysis results.

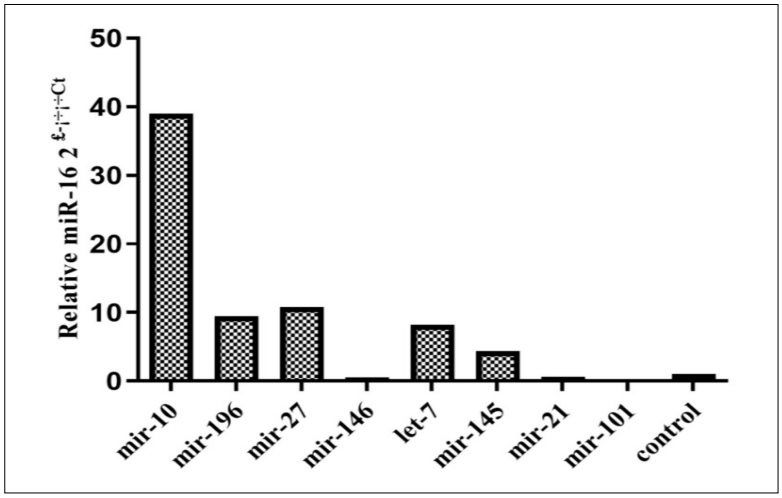

Fig 7: Validation of differential expression microRNA.

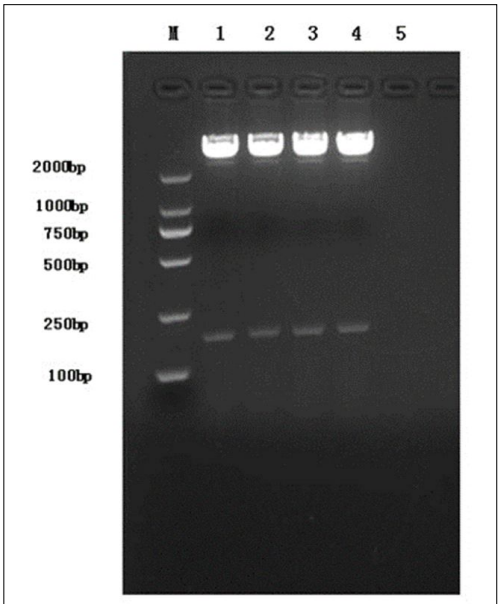

M: DL-2000Marker 1-2: TLR-11 3'-UTR 3-4: TLR-11 mut-3'-UTR 5: double distilled water.

Fig 8: 1.5% agarose gel electrophoresis results.

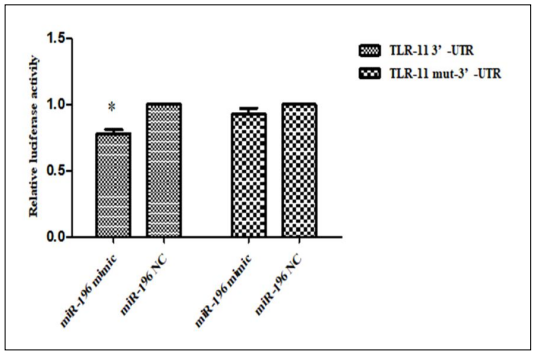

Fig 9: Expression of the TLR-11-3 '- UTR gene. *means P<0.05.

TLR-11 3′-UTR+miR-196 mimic and TLR-11 3′-UTR+miR-196 NC, the luciferase activity of TLR-11 3′-UTR+miR-196 mimic group decreased significantly (P<0.05) and the difference was significant. There was no significant difference in the activity expression of each group of fluorinase (P>0.05) in the comparison of plasmid TLR-11 mut-3′-UTR+miR-196 mimic and TLR-11 mut 3′-UTR+miR-196 NC of transfected recombinant vector as shown in Fig 9. It was proved that miR-196 could bind specifically to 3′UTR region of TLR-11 gene, which affected the expression of firefly fluorinase in plasmid, resulting in a significant decrease in the luminescence value of firefly in the test group. In turn, it is concluded that TLR-11 is the target gene of miR-196.

CONCLUSION

This study was conducted by using cutting-edge techniques like fluorescence quantitative PCR and high-throughput sequencing to analyze and identify MicroRNAs involved in *C. parvum* infection, to reveal their molecular mechanism at the RNA level and investigate the variation of microRNA in the body after *C. parvum* infection. Therefore, studying changes in intestinal epithelial miRNAs following *C.parvum* infection of the host will help us understand the mechanisms of host- *C. parvum* interactions.

ACKNOWLEDGEMENT

The present study was supported by Scientific Research Fund of Tangshan Normal University (20255129066); Tangshan Livestock and Poultry Intestinal Health Regulation Basic In Novation Team (23130234E); Special Fund for the Construction of Modern Agricultural Industry Technology System in Hebei Province (HBCT2024230201); Tangshan Experimental Station of the Innovation Team for Milk and Beef Cattle in the Modern Agricultural Industry Technology System of Hebei Province (HBCT202 3180403).

Disclaimers

The views and conclusions expressed in this article are solely those of the authors and do not necessarily represent the views of their affiliated institutions. The authors are responsible for the accuracy and completeness of the information provided, but do not accept any liability for any direct or indirect losses resulting from the use of this content.

Informed consent

All animal procedures for experiments were approved by the Committee of Experimental Animal Care and Handling Techniques were approved by the University of Animal Care Committee.

Conflict of interest

The authors declare that there are no conflicts of interest regarding the publication of this article. No funding or sponsorship influenced the design of the study, data collection, analysis, decision to publish, or preparation of the manuscript.

REFERENCES

Bouzid, M., Hunter, P.R., Chalmers, R.M. and Tyler, K.M. (2014). *Cryptosporidium* pathogenicity and virulence. *Clinical Microbiology Reviews*. **26(1):** 115-134.

Crawford, C.K. and Kol, A. (2021). The mucosal innate immune response to *Cryptosporidium parvum*, a global one health issue. *Frontiers in Cellular and Infection Microbiology*. **11:** 689401.

Deng, Z., Zhang, Y. and Li, L. (2022). A dual luciferase reporter system for characterization of small RNA target genes in both mammalian and insect cells. *Insect Science*. **29(3):** 631-644.

Dixit, P., Rao, M.L.V., Dixit, A.K., Gupta, R. and Shukla, P.C. (2019). Prevalence and molecular charac-terisation of Cryptosporidium spp. in goat kids. *Indian Journal of Animal Research*. **53(9):** 1234-1238. doi: 10.18805/ijar.B-3642.

Gallego, L.G., Mendoza, C.C. and Tibabuzo, P.A. (2022). Dual transcriptomics to determine gamma interferon-independent host response to intestinal *Cryptosporidium parvum* infection. *Infection and Immunity*. **90(2):** e63821.

Hu, G., Gong, A., Amanda, L.R. and Huang, B.Q. (2013). Release of luminal exosomes contributes to TLR4-mediated epithelial antimicrobial defense. *PLoS Pathogens*. **9(4):** e1003261.

Jeseninik, T., 'tajner, N., Radišek, S. and Mishra, A.K. (2022). Discovery of microRNA-like small RNAs in pathogenic plant fungus verticillium nonalfalfae using high-throughput sequencing and qPCR and RLM-RACE validation. *International Journal of Molecular Sciences*. **23(2):** 900.

Khandelwal, V., Sharma, T., Choudhary, P. and Gupta, S. (2024). MicroRNAs: An important signature molecule to improve health and welfare in livestock: A review. *Indian Journal of Animal Research*. **58(2):** 179-189. doi: 10.18805/IJAR.B-5231.

Li, T., Liu, H., Jiang, N. and Wang, Y. (2021). Compamiceive proteomics reveals *Cryptosporidium parvum* manipulation of the host cell molecular expression and immune response. *PLoS Neglected Tropical Diseases*. **15(11):** e9949.

Nahand, J.S., Shojaie, L., Akhlagh, S.A. and Ebrahimi, M.S. (2021). Cell death pathways and viruses: Role of microRNAs. *Molecular Therapy-nucleic Acids*. **24:** 487-511.

Rider, S.D. and Zhu, G. (2010). *Cryptosporidium*: Genomic and biochemical features. *Experimental Parasitology*. **124(1):** 2-9.

Shaw, H.J., Armstrong, C., Uttley, K. and Morrison, L.J. (2021). Genetic diversity and shedding profiles for *Cryptosporidium parvum* in adult cattle and their calves. *Current Research in Parasitology and Vector-Borne Diseases*. **1:** 100027.

Xiao, X., Mao, X., Chen, D.W. and Yu, B. (2022). miRNAs can affect intestinal epithelial barrier in inflammatory bowel disease. *Frontiers in Immunology*. **13:** 863229.

Xie, H., Lei, N., Gong, A., Xian-Ming, C.b. and Hu, G. (2014). *Cryptosporidium parvum* induces SIRT1 expression in host epithelial cells through downregulating let-7i. *Human Immunology*. **75(8):** 760-765.

Xie, F., Zhang, Y., Li, J. and Sun, L. (2022). MiR-942-5p targeting the IFI27 gene regulates HCT-8 cell apoptosis *via* a TRAIL-dependent pathway during the early phase of *Cryptosporidium parvum* infection. *Parasites and Vectors*. **15(1):** 291.

Xie, X., Pang, M. and Liang, S. (2021). Cellular microRNAs influence replication of H3N2 canine influenza virus in infected cells. *Veterinary Microbiology*. **257:** 109083.

Yin, H., Xiaqing, S., Liu, J., Li, L., Tian, Y. and Peng, J. (2021). Potential effect of β-casomorphin-7 on lymphocyte and tlr\NF-κb signaling pathway in intestinal mucosa of aged mice. *Indian Journal of Animal Research*. **55(7):** 791-795. doi: 10.18805/ijar. B-1215.

Zolova, A., Keidâne, D. and Zolovs, M. (2022). Prevalence of susceptibility to *Cryptosporidium spp*. among dairy calves with different feeding regimens with an emphasis on the feeding of transition milk. *Veterinary World*. **15(5):** 1256-1260.